



RESEARCH LETTER

10.1002/2016GL069119

Key Points:

- Discrimination between Eastern and Central Pacific El Niño
- New index based on climate networks for objective classification
- Discriminations are possible for La Niña as well

Correspondence to:

M. Wiedermann,
marcwie@pik-potdam.de

Citation:

Wiedermann, M., A. Radebach, J. F. Donges, J. Kurths, and R. V. Donner (2016), A climate network-based index to discriminate different types of El Niño and La Niña, *Geophys. Res. Lett.*, 43, 7176–7185, doi:10.1002/2016GL069119.

Received 13 APR 2016

Accepted 20 MAY 2016

Accepted article online 27 MAY 2016

Published online 14 JUL 2016

A climate network-based index to discriminate different types of El Niño and La Niña

Marc Wiedermann^{1,2}, Alexander Radebach^{3,4}, Jonathan F. Donges^{1,5},
Jürgen Kurths^{1,2,6,7}, and Reik V. Donner¹

¹Potsdam Institute for Climate Impact Research, Potsdam, Germany, ²Department of Physics, Humboldt University, Berlin, Germany, ³Mercator Research Institute on Global Commons and Climate Change, Berlin, Germany, ⁴Economics of Climate Change, Technical University, Berlin, Germany, ⁵Stockholm Resilience Centre, Stockholm University, Stockholm, Sweden, ⁶Institute for Complex Systems and Mathematical Biology, University of Aberdeen, Aberdeen, UK, ⁷Department of Control Theory, Nizhny Novgorod State University, Nizhny Novgorod, Russia

Abstract El Niño exhibits distinct Eastern Pacific (EP) and Central Pacific (CP) types which are commonly, but not always consistently, distinguished from each other by different signatures in equatorial climate variability. Here we propose an index based on evolving climate networks to objectively discriminate between both flavors by utilizing a scalar-valued measure that quantifies spatial localization and dispersion in global teleconnections of surface air temperature. Our index displays a sharp peak (high localization) during EP events, whereas during CP events (larger dispersion) it remains close to the values observed during normal periods. In contrast to previous classification schemes, our approach specifically accounts for El Niño's global impacts. We confirm recent El Niño classifications for the years 1951 to 2014 and assign types to those cases where former works yielded ambiguous results. Ultimately, we demonstrate that our index provides a similar discrimination of La Niña episodes into two distinct types.

1. Introduction

The El Niño–Southern Oscillation (ENSO) alternates between positive (El Niño) and negative (La Niña) phases [Trenberth, 1997]. Especially the El Niño phase further exhibits two distinct types characterized by different spatial patterns of sea surface temperature (SST) anomalies [e.g., Ashok et al., 2007; Kao and Yu, 2009; Kug et al., 2009; Yeh et al., 2009]. The first type (the classic or Eastern Pacific (EP) El Niño [Rasmusson and Carpenter, 1982; Harrison and Larkin, 1998]) is characterized by strong positive SST anomalies close to the western coast of South America, while the second type (referred to as El Niño Modoki or Central Pacific (CP) El Niño by different authors) exhibits the strongest SST anomalies close to the dateline. Both types cause different impacts on the global climate system, such as increased rainfall over northern and eastern Australia during CP El Niños [Ashok et al., 2007; Taschetto and England, 2009] contrasted by a rainfall reduction over eastern Australia during EP El Niños [Chiew et al., 1998]. Thus, a proper discrimination of these types provides key information to assess El Niño's possible impacts on other climate subsystems.

While recent literature shows a large agreement on the classification of many El Niños, contradictory classifications arise in certain years such as, e.g., 1986/1987, which has been classified as mixed [Kug et al., 2009], EP [Kim et al., 2011; Yeh et al., 2009; Hu et al., 2011] or CP [Larkin and Harrison, 2005; Hendon et al., 2009; Graf and Zanchettin, 2012]. In fact, when reviewing existing studies [Kim et al., 2009; Kug et al., 2009; Kim et al., 2011; Yeh et al., 2009; Hu et al., 2011; Larkin and Harrison, 2005; Hendon et al., 2009; Graf and Zanchettin, 2012], 8 out of 19 El Niño events between 1957 and 2010 have not been classified in agreement. These mismatches possibly arise since most discrimination schemes utilize the same observable (mostly SST) but apply different derived characteristics such as the ENSO Modoki Index (EMI) [Ashok et al., 2007], the Nino3 index and Nino4 index [Kim et al., 2011; Hu et al., 2011], or empirical orthogonal function (EOF) analysis [Kao and Yu, 2009; Graf and Zanchettin, 2012] to distinguish both El Niño types. Specifically, the latter requires some manual thresholding of the EOFs' time evolution which may result in ambiguous classifications that strongly depend on the choice of the threshold.

To provide a consistent and systematic discrimination, we propose here a method to distinguish the two different El Niño types based on the assessment of time evolving complex climate networks [Radebach *et al.*, 2013]. By incorporating statistics of higher order, it produces a sharp signal compared to first-order statistics such as mean values or EOF analysis and simultaneously retains a manageable number of parameters that can be well related to ENSO's spatiotemporal properties.

Climate networks consist of nodes representing time series and links displaying some statistically relevant interdependency between them [Donges *et al.*, 2009a; Tsonis *et al.*, 2006]. ENSO has been studied intensively using this tool to quantify corresponding teleconnections [Gozolchiani *et al.*, 2011; Tsonis and Swanson, 2008; Tsonis *et al.*, 2008], its effect on other climatic subsystems [Gozolchiani *et al.*, 2008], and the dynamics of its related oceanic wave dynamics [Wang *et al.*, 2016]. Additionally, climate network approaches allowed successfully forecasting El Niño by assessing the strength of linkages in the equatorial Pacific [Ludescher *et al.*, 2013, 2014].

Radebach *et al.* [2013] systematically studied the temporal evolution of a global climate network in a spatially explicit way and linked the resulting variability of its topology to the presence of the two different El Niño types. Following upon these results, we develop a thorough classification scheme that allows for an objective discrimination between EP and CP El Niños. While most previous studies on El Niño classification focus on climate variability only within the equatorial Pacific, we specifically acknowledge the global impact of ENSO. Our framework therefore accounts for the correlation structure of global surface air temperature anomalies (SATA), a variable that is highly affected by El Niño [Yamasaki *et al.*, 2008] and is, in contrast to SST, available homogeneously sampled for the entire globe.

As an index that discriminates EP and CP El Niños, we utilize the climate network's transitivity, a scalar-valued measure that quantifies the (disperse versus strongly localized) spatial distribution of pairwise correlations and teleconnections around the globe. First, we assess whether a certain period displays El Niño conditions according to the Oceanic Niño Index (ONI). Second, we determine the transitivity of evolving climate networks computed from 1 year running-window cross correlations with respect to a baseline value defined by the transitivity of networks computed from 30 year windows that are centered around the period of interest. The surpassing of that threshold defines an EP El Niño, while the opposite case indicates a CP El Niño. In comparison with recent studies, our methods confirms all EP and CP El Niños between 1951 and 2014 that were commonly defined by Kug *et al.* [2009], Kim *et al.* [2011], Yeh *et al.* [2009], Hu *et al.* [2011], Larkin and Harrison [2005], Hendon *et al.* [2009], and Graf and Zanchettin [2012] and provides a consistent assignment for those periods that were ambiguously classified so far.

To consolidate our findings, we provide results for the climate network's node strength fields during periods that our index defines as EP or CP El Niños and show their similarity with patterns that are expected from an EOF analysis [Johnson, 2013; Donges *et al.*, 2015a]. As recent works [Kug and Ham, 2011; Yuan and Yan, 2012; Tedeschi *et al.*, 2013] addressed the issue whether two types of La Niña can be detected as well, we perform the same procedure for these events and provide a similar discrimination for the negative phase of ENSO.

2. Data

We define El Niño periods according to the Oceanic Niño Index (ONI) provided by the Climate Prediction Center of the National Oceanic and Atmospheric Administration, which covers the time between 1950 and 2015 and is computed as the 3 month running mean SST anomaly in the Niño3.4 region (5°N–5°S, 120°W–170°W) with respect to centered 30 year base periods that are updated every 5 years. As the initial year and final year of this data set include only incomplete information on the 1951 La Niña and the 2015 El Niño, we restrict ourselves to the period from 1951 to 2014.

We construct evolving climate networks from daily global surface air temperature (SAT) data provided by the National Centers for Environmental Prediction (NCEP)/National Center for Atmospheric Research (NCAR) reanalysis [Kalnay *et al.*, 1996] with a spatial resolution of 2.5° in longitudinal and latitudinal direction covering the same time period as the ONI. All 288 grid points located at the poles and all leap days are removed. The data are anomalized in accordance with the definition of the ONI by subtracting from the time series at every grid point the long-term annual cycle computed over the same 30 year base periods as above that are updated every 5 years. Due to the lack of data before 1948 and after 2015, the years 1951 to 1965 are anomalized by the same base period (1951–1980) as the years 1965 to 1969. Similarly, the years 2005 to 2015 are anomalized

by the 1986 to 2015 base period. We note that this procedure induces small offsets in the time series after every 5 years. However, as we construct evolving climate networks from time series of much shorter length, we neglect these effects for the sake of consistency with the definition of the ONI. The above anomalization process ensures that once defined anomalies and ENSO periods are not altered by the addition of more recent data.

Finally, we obtain $N=10,224$ time series $x_i(t)$ of surface air temperature anomalies (SATA) with $N_t=23,360$ temporal sampling points each.

3. Methods

A climate network G consists of a set of N nodes that correspond to the grid points in the underlying data set and a set of M links which connect pairs of nodes and indicate a strong statistical interrelationship between them. The network is represented by its binary adjacency matrix \mathbf{A} with entries $A_{ij} = 1$ if two nodes i and j are linked and $A_{ij} = 0$ otherwise [Donges et al., 2009b; Boers et al., 2013; Stolbova et al., 2014]. An extension of this procedure is the usage of an edge-weighted adjacency matrix \mathbf{W} where $W_{ij} = 0$ denotes the absence of a link, but $W_{ij} > 0$ denotes its strength (e.g., the pairwise correlation) [Barrat et al., 2004; Hlinka et al., 2014; Zemp et al., 2014].

3.1. Network Construction

Following the framework of evolving climate network analysis [Radebach et al., 2013; Hlinka et al., 2014], we construct a sequence of networks G_n from running-window cross-correlation matrices $\mathbf{C}_n = (C_{n,ij})$ between all pairs of SATA time series. A window n is characterized by its size w and offset d to the previous window. We choose $d = 30$ days and $w = 365$ days to ensure that each window covers at least the entire duration of an El Niño or La Niña episode. For each window n we obtain the truncated time series $\{x_{n,i}(t_n)\}$, $t_n = \{nd, nd + 1, \dots, nd + w - 1\}$ and compute the resulting $N \times N$ cross-correlation matrix \mathbf{C}_n . In accordance with previous studies that utilized either monthly [Donges et al., 2009a; Tsonis et al., 2006; Paluš et al., 2011] or daily [Radebach et al., 2013] data, we rely here on the linear Pearson correlation at zero lag.

To reduce the complexity of \mathbf{C}_n , it is advisable to represent only a certain fraction ρ of strongest absolute correlations as links between the nodes [Tsonis et al., 2006; Donges et al., 2009a]. This yields an individual threshold T_n for each absolute correlation matrix $\mathbf{C}_n^{\text{abs}} = (|C_{n,ij}|)$ above which nodes are treated as linked. ρ is then called the *link density* of G_n . Here we keep $\rho = 0.005$ fixed for all windows n . This choice gives a number of M links low enough to ensure the consideration of only the strongest correlations. Further, $\rho = 0.005$ roughly corresponds to the fraction of nodes that are situated inside the Niño3.4 region. We obtain thresholds (i.e., the lower bound of absolute correlations values) T_n in the range of 0.53 to 0.65. They are significant above the 99% significance level according to a standard Student's t test.

Taken together, the construction of evolving climate networks depends on only two parameters: window size w and link density ρ . Compared to, e.g., the EMI which requires at least the weights of its three contributions to be fixed, the number of parameters in our framework is (i) of comparable order and (ii) each parameter can be selected in a meaningful way according to ENSO's temporal (window size w) and spatial extent (link density ρ).

Binarizing $\mathbf{C}_n^{\text{abs}}$ to an edge-unweighted adjacency matrix \mathbf{A}_n would neglect valuable information on the varying strength of correlation between connected grid points. We therefore compute edge-weighted adjacency matrices \mathbf{W}_n with entries $|C_{n,ij}|$ if two nodes i and j are linked,

$$W_{n,ij} = |C_{n,ij}| \cdot \Theta(|C_{n,ij}| - T_n). \tag{1}$$

Due to the underlying grid type, the density of nodes increases toward the poles inducing a systematic bias into the computation of network measures [Heitzig et al., 2012]. This effect is corrected by assigning each node a weight w_i corresponding to its latitudinal position λ_i on the grid [Tsonis et al., 2006; Heitzig et al., 2012; Wiedermann et al., 2013],

$$w_i = \cos(\lambda_i), \tag{2}$$

resulting in so-called *node splitting invariant* measures [Heitzig et al., 2012; Zemp et al., 2014; Wiedermann et al., 2013].

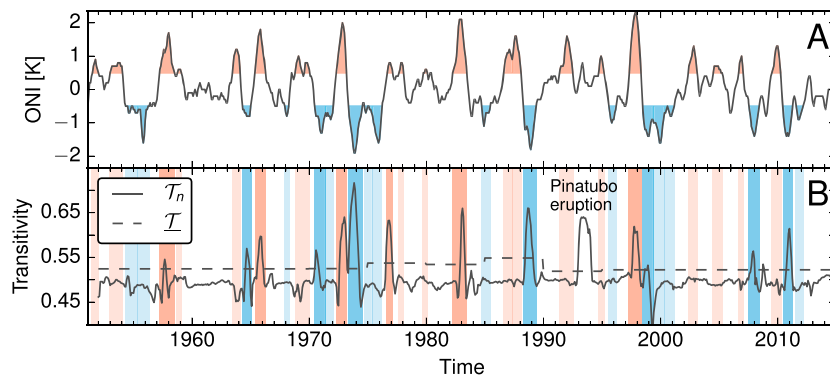


Figure 1. (a) The ONI with El Niño (La Niña) periods marked in red (blue). (b) Time evolution of the evolving climate network's transitivity \mathcal{T}_n . The dashed horizontal line indicates the baseline transitivity $\underline{\mathcal{T}}$. Colored areas highlight El Niño and La Niña periods. Darker coloring indicates those periods where \mathcal{T}_n exceeds $\underline{\mathcal{T}}$ and that are thus classified as EP type.

3.2. Network Transitivity

El Niño has a global impact on the climate system manifested by long-ranging teleconnections with different regions of the Earth [Held et al., 1989; Neelin, 2003; Trenberth, 1997] which, in the context of climate networks, can be regarded as mediators of variations and fluctuations [Tsonis et al., 2008; Runge et al., 2015]. Thus, El Niño and its teleconnections cause a spatial organization of high covariability along the Earth's surface, which is reflected in the resulting climate network. The degree of this organization can be quantified by a single-valued scalar metric, the network transitivity [Watts and Strogatz, 1998; Saramäki et al., 2007], which we use in its node-weighted form [Heitzig et al., 2012],

$$\mathcal{T}_n = \frac{\sum_{i,j,k} w_i W_{n,ij} w_j W_{n,jk} w_k W_{n,ki}}{\sum_{i,j,k} w_i W_{n,ij} w_j W_{n,jk} w_k} \in [0, 1]. \quad (3)$$

\mathcal{T}_n gives the edge- and node-weighted fraction of completely linked triples of nodes and measures how strongly the correlation in a system under study or subsets thereof is spatially organized (high values) or dispersed (low values). In a purely random network, \mathcal{T}_n would naturally take very low values, i.e., approximately equal to the link density in the standard case of no specific edge and node weights [Erdős and Rényi, 1960]. \mathcal{T}_n thus serves as a good discriminator between phases of strong localization and high dispersion in the global teleconnectivity of evolving climate networks [Radebach et al., 2013]. As EP and CP El Niños have been shown to display different characteristics in their associated teleconnections [Ashok et al., 2007], we expect \mathcal{T}_n to respond differently to the presence of either of the two types.

3.3. Strength of Individual Nodes

To connect our work with previous results from statistical climatology, we investigate for each node i its corresponding area-weighted strength

$$s_{n,i} = \sum_j w_j W_{n,ij} \quad (4)$$

individually for each network G_n . $s_{n,i}$ measures the total weight of links that are attached to each node i . For the edge-unweighted case, this measure reduces to the area-weighted connectivity [Tsonis et al., 2008] which displays striking similarity with results from a node-weighted EOF analysis [Donges et al., 2015a; Wiedermann et al., 2015].

4. Results

The ONI identifies El Niño (La Niña) episodes if its values exceed (fall below) a threshold of 0.5 K (−0.5 K) for at least five consecutive months, yielding 22 (18) El Niño (La Niña) episodes between 1951 and 2014 (Figure 1a).

4.1. Transitivity

We construct $n = 733$ evolving climate networks and compute their transitivity \mathcal{T}_n and node strength $s_{n,i}$. The end point of each window marks the time at which the two measures are evaluated. Figure 1b shows the

evolution of \mathcal{T}_n . Except for one case with several 12 month time windows ending in 1993, which reflects large-scale spatially coherent cooling after the Mount Pinatubo eruption in 1991 [McCormick *et al.*, 1995; Radebach *et al.*, 2013], peaks in \mathcal{T}_n coincide exclusively with distinct ENSO episodes. As shown by Radebach *et al.* [2013], the presence of an EP El Niño likely coincides with strong signals in (for their case unweighted) transitivity, while no distinct signal is present during CP El Niños. However, no quantitative criterion for this discrimination has been given so far.

To give an objective definition of a *strong* transitivity signal, we define a threshold value $\underline{\mathcal{T}}$ above which \mathcal{T}_n is considered to display a peak. We obtain an adaptive value of $\underline{\mathcal{T}}$ as the transivities of climate networks constructed for the same 30 year periods that were used for the anomalization of the SAT data and the derivation of the ONI. Thus, we compare all values of \mathcal{T}_n computed, e.g., during the period 1975–1979 with a baseline transitivity $\underline{\mathcal{T}}$ computed for a climate network covering the 30 year period of 1961–1990 (dashed line in Figure 1b). This procedure follows the definition of the ONI, and we interpret $\underline{\mathcal{T}}$ as representing the long-term average spatial organization in the global climate network. Adaptively updating $\underline{\mathcal{T}}$ every 5 years automatically accounts for possible effects of long-term trends imprinting on the network statistics, and the definition of $\underline{\mathcal{T}}$ for periods in the past is not affected by the addition of more recent data.

We detect six El Niño periods during which \mathcal{T}_n exceeds $\underline{\mathcal{T}}$ (dark red areas in Figure 1b) corresponding to the El Niños of 1957, 1965, 1972, 1976, 1982, and 1997. For all other El Niños \mathcal{T}_n stays below $\underline{\mathcal{T}}$. In the scope of our framework, we thus propose classifying the first case as EP and the second case as CP events (light red areas in Figure 1b).

For comparison, the proposed classifications of El Niño phases into EP and CP types from eight recent studies [Kim *et al.*, 2009; Kug *et al.*, 2009; Kim *et al.*, 2011; Yeh *et al.*, 2009; Hu *et al.*, 2011; Larkin and Harrison, 2005; Hendon *et al.*, 2009; Graf and Zanchettin, 2012] are summarized in Table 1. To quantify the consistency of the network-based discrimination, we define a true positive rate (TPR) as the fraction of EP El Niños in each study that are detected by our framework. Accordingly, the false positive rate (FPR) is the fraction of CP El Niños in each study that our method classifies as EP type. With respect to all references we obtain a FPR of zero. The TPR for each reference is presented in the last row of Table 1. Its values vary between 1 for the comparison with Graf and Zanchettin [2012] and Hu *et al.* [2011], and 0.5 for the comparison with Yeh *et al.* [2009]. Furthermore, we note that among all references 8 out of 19 events are not classified in agreement. Taking only the mutual agreement between all references as a basis for testing, we confirm all past classifications (second to last column in Table 1). To provide results for the eight ambiguously defined periods, the network-based classification for all El Niños is given in the last column of Table 1.

We find the largest consistency with the results from Graf and Zanchettin [2012] which are obtained from an EOF analysis, a framework that, like our method, is based on the evaluation of cross correlations between different grid points. This methodological congruence may explain the good agreement between the results and confirms the validity of our work. However, by utilizing a network-based approach instead of EOFs, the entire spatial structure of the underlying covariance patterns is reduced to a single index. Its evaluation does not rely on any visual inspection but provides an objective binary classification depending on whether or not the short-term transitivity \mathcal{T}_n exceeds its long-term baseline $\underline{\mathcal{T}}$.

We repeat the analysis for La Niña periods and classify 7 EP (1964, 1970, 1973, 1988, 1998, 2007, and 2010) and 11 CP (1954, 1955, 1967, 1971, 1974, 1975, 1984, 1995, 2000, 2001, and 2011) periods (dark (EP) and light (CP) blue areas in Figure 1b). Even though references providing actual discriminations of the different La Niña years are scarce, we compiled two recent works and confirm the reported EP La Niñas of 1964 and 1970 [Yuan and Yan, 2012] and CP La Niñas of 1975, 1984, 2000, 2001, and 2011 [Yuan and Yan, 2012; Tedeschi *et al.*, 2013]. Future work should further evaluate the discrimination of La Niña periods proposed by our method.

4.2. Node Strength

To further consolidate our findings, we compute the average node strengths $s_{B,i}$ from the six networks that are used to define $\underline{\mathcal{T}}$ (Figure 2a). We obtain the highest values in the equatorial Pacific highlighting ENSO's importance in the global climate network. Additionally, we compute the average node strength $s_{N,i}$ taken over all *normal* periods, i.e., those periods where neither El Niño or La Niña are present (Figure 2b). As by its definition the effect of ENSO is reduced and $s_{N,i}$ displays comparably low values and a relatively homogeneous distribution across the entire globe as compared to $s_{B,i}$. Ultimately, we calculate the average node strength $s_{ENEP,i}$ ($s_{ENCP,i}$) taken over all El Niño periods that our method classifies as EP (CP) type (see also Figure 1b).

Table 1. Recent Classifications of El Niño Phases Into CP and EP Episodes^a

	<i>Kug et al.</i> [2009]	<i>Kim et al.</i> [2011]	<i>Hu et al.</i> [2011]	<i>Larkin et al.</i> [2005]	<i>Hendon et al.</i> [2009]	<i>Graf et al.</i> [2012]	<i>Yeh et al.</i> [2009]	<i>Kim et al.</i> [2009]	Literature Synthesis	This study
1953/1954	-	-	-	-	-	-	-	-	-	CP
1957/1958	-	-	EP	EP	-	EP	EP	EP	EP	EP
1958/1959	-	-	-	-	-	-	-	-	-	CP
1963/1964	-	-	-	CP	-	CP	EP	EP	-	CP
1965/1966	-	-	EP	EP	-	EP	EP	EP	EP	EP
1968/1969	-	-	CP	CP	-	CP	CP	-	CP	CP
1969/1970	-	-	EP	EP	-	-	EP	CP	-	CP
1972/1973	EP	EP	EP	EP	-	EP	EP	EP	EP	EP
1976/1977	EP	EP	-	EP	-	EP	EP	EP	EP	EP
1977/1978	CP	CP	-	CP	-	CP	CP	-	CP	CP
1979/1980	-	-	-	-	-	-	b	-	-	CP
1982/1983	EP	EP	EP	EP	EP	EP	EP	EP	EP	EP
1986/1987	b	EP	EP	CP	CP	CP	EP	-	-	CP
1987/1988	b	-	CP	EP	EP	-	EP	EP	-	CP
1991/1992	b	EP	EP	EP	CP	CP	EP	CP	-	CP
1994/1995	CP	CP	CP	CP	CP	CP	CP	CP	CP	CP
1997/1998	EP	EP	EP	EP	EP	EP	EP	EP	EP	EP
2002/2003	CP	CP	CP	EP	CP	CP	b	CP	-	CP
2004/2005	CP	CP	-	-	CP	CP	CP	CP	CP	CP
2006/2007	-	EP	CP	CP	-	-	EP	-	-	CP
2009/2010	-	CP	-	-	-	CP	-	-	CP	CP
TPR	1.0	0.57	0.62	0.6	0.67	1.0	0.5	0.75	1.0	

^aA hyphen denotes that no classification was performed for the specific year. Bold letters denote events where the network-based classification is in agreement with the reference. The last row summarizes the true positive rate (TPR) of our formalism. The second to last column indicates agreement of existing studies, and the last column summarizes the classification obtained from the network-based approach.

^bMixed or undefined states.

To investigate the deviation from the normal state during either of the two periods, we display their differences from $s_{N,i}$ in Figures 2c and 2d. For EP El Niños (Figure 2c) we find an expected maximum in the equatorial Pacific, which is the typical ENSO-related pattern known from classical EOF analysis [Johnson, 2013]. For CP El Niños we find a weakening of this pattern and a westward shift of the maxima toward the dateline. This pattern has been observed in the corresponding EOFs as well [Johnson, 2013]. However, we note that $s_{ENCP,i}$ only differs from $s_{N,i}$ to a small amount (Figure 2d). This again suggests that during CP El Niños the evolving climate networks exhibit a similar state as during normal periods. We compute similar average quantities, $s_{LNEP,j}$ and $s_{LNEP,i}$, for La Niña events and again evaluate their deviations from the normal state (Figures 2e and 2f). We find quantitatively and qualitatively similar patterns as for El Niño, which highlights the symmetry of the two ENSO phases. Even though a similarly thorough comparison with existing literature is not yet possible for La Niña, the high congruence between $s_{ENEP,i}$ and $s_{LNEP,i}$ ($s_{ENCP,i}$ and $s_{LNEP,i}$) suggests that our discrimination scheme provides reasonable results for La Niña phases as well.

4.3. Robustness

To evaluate the robustness of our results with respect to the window size w and link density ρ , we vary both parameters individually and assess the difference between the TPR and FPR when testing our classification against the largest overlap of the literature (second to last column in Table 1). This score takes its maximum value of 1 if our method confirms the literature's classification of each event and is lower otherwise. Figure 3a (Figure 3b) shows the score for different w (ρ) and fixed $\rho=0.005$ ($w=365$ days). The highest scores are obtained for window sizes between $w=365$ and $w=547$ days and link densities between $\rho=0.005$ and $\rho=0.0075$. Shorter window sizes cause a reduction of the score as the windows become too small to sufficiently cover the temporal extent of an ENSO episode. For larger window sizes the effect of ENSO is suppressed

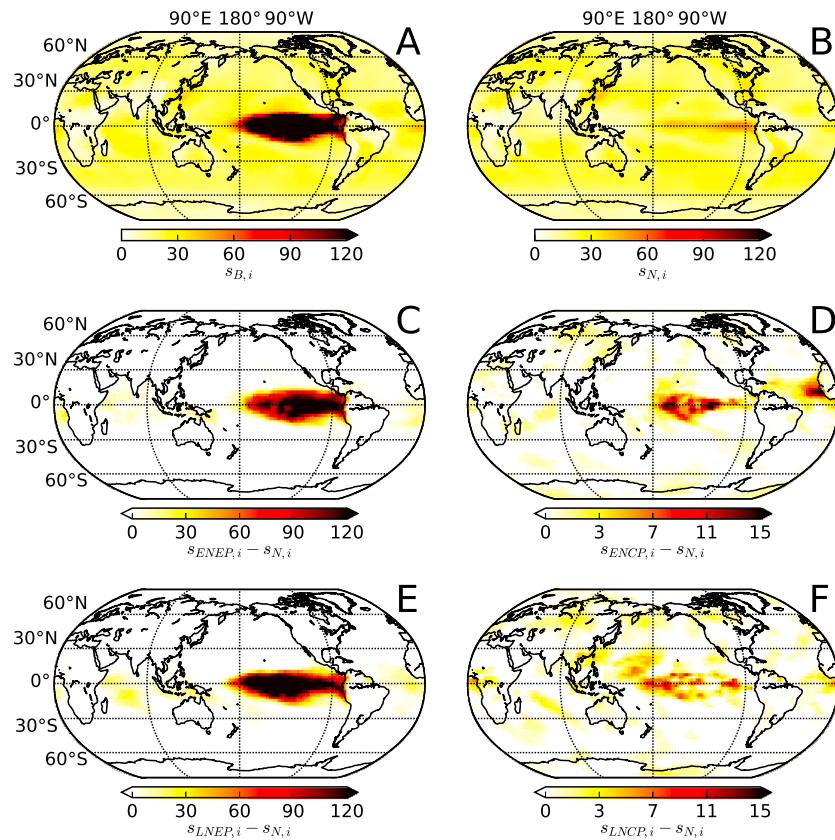


Figure 2. (a) Average strength of nodes in the baseline climate networks. (b) Average node strength of the evolving networks during normal periods. (c) Differences between the average node strength during El Niño periods that are classified as EP type and the average node strength during normal periods. (d) The same as in Figure 2c for El Niño periods that are classified as CP type. (e, f) The same as in Figures 2c and 2d for La Niña periods. Note the different color ranges in Figures 2c and 2e, and 2d and 2f, respectively.

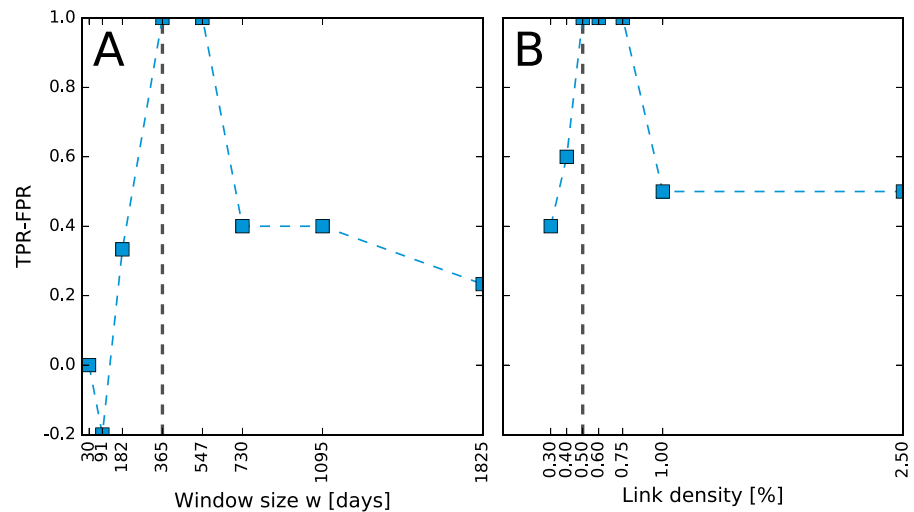


Figure 3. (a) Difference between true positive rate (TPR) and false positive rate (FPR) for classifications obtained from the network approach and the largest overlap between all references in Table 1 for different window sizes w and fixed link density $\rho=0.005$. (b) The same as in Figure 3a for different link densities ρ and fixed window size $w=365$ days. Dashed vertical lines indicate the choices of parameters that yield the results in Figures 1b and 2.

by including too many of the normal periods into each window. The link density of $\rho = 0.005$ was initially chosen as it roughly corresponds to the fraction of nodes located inside the Niño3.4 region. Smaller values cause the network to be only composed of highly correlated trivial nearest-neighbor connections and teleconnections with comparably lower pairwise cross-correlation values are not captured. In contrast, larger values result in too many trivial links alongside those attributed to the effects of ENSO. Generally, the score varies smoothly along the range of parameters and shows maximum values for our initial choices. Thus, we consider our results to be sufficiently robust.

5. Conclusion

We have proposed an index based on evolving climate networks to objectively discriminate between EP and CP types of El Niño and La Niña episodes. It relies on the evolution of the networks' transitivity, measuring spatial localization and dispersion of strong cross correlations between different grid points in a global SATA field. If this index peaks during a distinct ENSO phase, it detects the presence of an EP-type event. In contrast, the absence of a remarkable signal during an ENSO period indicates CP-type events. From the climate network perspective this indicates an increased localization and clustering of teleconnections during EP phases in comparison with CP and normal phases where teleconnections seem to appear more dispersed. Our method does not require any visual inspection or manual thresholding of observed patterns but objectively categorizes ENSO phases into different types by intercomparing the networks' short-term (\mathcal{T}_n) and long-term states (\mathcal{T}).

In comparison with eight recent works on El Niño classification our method confirms the classification of years that all references have in common and provides a discrimination for those years that were so far ambiguously defined. Unlike approaches based on the evaluation of (average) SST fields or first-order statistics thereof our method produces a sharp and distinct signal in the variable under study, i.e., the network transitivity, and thus provides a clear distinction between the two types of El Niño episodes.

Even though references are scarce, our findings also confirm different recently reported EP and CP La Niña periods and show that our discrimination scheme is applicable to this negative phase of ENSO as well.

In summary, our method is a meaningful complement to existing frameworks as it (i) proposes objective classifications where former work yielded ambiguous results and (ii) depends only on a low number of parameters which can be estimated from ENSO's well-studied spatiotemporal extent, while (iii) showing no larger computational complexity than EOF-based methods. Further, we show that the exact choice of parameters does not affect the outcome of the analysis as long as they are varied over a climatologically reasonable range.

Future work should investigate more thoroughly the spatial distribution of links in the evolving climate networks during different ENSO stages to gain a more systematic understanding of the physical mechanisms behind the observed differences in transitivity. Moreover, being automated and objective, our framework allows for a systematic evaluation of climate model simulations and could be used to investigate potential changes in the projected frequency of the two ENSO flavors in the future, e.g., due to anthropogenic global warming [Yeh *et al.*, 2009].

Acknowledgments

M.W. and R.V.D. have been supported by the German Federal Ministry for Education and Research via the BMBF Young Investigators Group CoSy-CC² (grant 01LN1306A). J.F.D. thanks the Stordalen Foundation via the Planetary Boundary Research Network (PB.net) and the Earth League's EarthDoc program for financial support. J.K. acknowledges the IRTG 1740 funded by DFG and FAPESP. NCEP Reanalysis data are provided by the NOAA/OAR/ESRL PSD, Boulder, Colorado, USA, from their website <http://www.esrl.noaa.gov/psd/>. Parts of the analysis have been performed using the Python package `pyunicorn` [Donges *et al.*, 2015b] available at <https://github.com/pik-copan/pyunicorn>.

References

- Ashok, K., S. K. Behera, S. A. Rao, H. Weng, and T. Yamagata (2007), El Niño Modoki and its possible teleconnection, *J. Geophys. Res.*, *112*, C111007, doi:10.1029/2006JC003798.
- Barrat, A., M. Barthélemy, R. Pastor-Satorras, and A. Vespignani (2004), The architecture of complex weighted networks, *Proc. Natl. Acad. Sci. USA*, *101*(11), 3747–3752, doi:10.1073/pnas.0400087101.
- Boers, N., B. Bookhagen, N. Marwan, J. Kurths, and J. Marengo (2013), Complex networks identify spatial patterns of extreme rainfall events of the South American Monsoon System, *Geophys. Res. Lett.*, *40*(16), 4386–4392, doi:10.1002/grl.50681.
- Chiew, F. H. S., T. C. Piechota, J. A. Dracup, and T. A. McMahon (1998), El Niño/Southern Oscillation and Australian rainfall, streamflow and drought: Links and potential for forecasting, *J. Hydrol.*, *204*(14), 138–149, doi:10.1016/S0022-1694(97)00121-2.
- Donges, J. F., Y. Zou, N. Marwan, and J. Kurths (2009a), Complex networks in climate dynamics, *Eur. Phys. J. Spec. Top.*, *174*(1), 157–179, doi:10.1140/epjst/e2009-01098-2.
- Donges, J. F., Y. Zou, N. Marwan, and J. Kurths (2009b), The backbone of the climate network, *Europhys. Lett.*, *87*(4), 48007, doi:10.1209/0295-5075/87/48007.
- Donges, J. F., I. Petrova, A. Loew, N. Marwan, and J. Kurths (2015a), How complex climate networks complement eigen techniques for the statistical analysis of climatological data, *Clim. Dyn.*, *9*(45), 2407–2424, doi:10.1007/s00382-015-2479-3.
- Donges, J. F., *et al.* (2015b), Unified functional network and nonlinear time series analysis for complex systems science: The `pyunicorn` package, *Chaos*, *25*(11), 113101, doi:10.1063/1.4934554.
- Erdős, P., and A. Rényi (1960), On the evolution of random graphs, *Publ. Math. Inst. Hung. Acad. Sci.*, *5*, 17–61.

- Gozolchiani, A., K. Yamasaki, O. Gazit, and S. Havlin (2008), Pattern of climate network blinking links follows El Niño events, *Europhys. Lett.*, *83*(2), 28005, doi:10.1209/0295-5075/83/28005.
- Gozolchiani, A., S. Havlin, and K. Yamasaki (2011), Emergence of El Niño as an autonomous component in the climate network, *Phys. Rev. Lett.*, *107*(14), 148501, doi:10.1103/PhysRevLett.107.148501.
- Graf, H.-F., and D. Zanchettin (2012), Central Pacific El Niño, the subtropical bridge, and Eurasian climate, *J. Geophys. Res.*, *117*(D1), D01102, doi:10.1029/2011JD016493.
- Harrison, D. E., and N. K. Larkin (1998), El Niño–Southern Oscillation sea surface temperature and wind anomalies, 1946–1993, *Rev. Geophys.*, *36*(3), 353–399, doi:10.1029/98RG00715.
- Heitzig, J., J. F. Donges, Y. Zou, N. Marwan, and J. Kurths (2012), Node-weighted measures for complex networks with spatially embedded, sampled, or differently sized nodes, *Eur. Phys. J. B*, *85*(1), 1–22, doi:10.1140/epjb/e2011-20678-7.
- Held, I. M., S. W. Lyons, and S. Nigam (1989), Transients and the extratropical response to El Niño, *J. Atmos. Sci.*, *46*(1), 163–174, doi:10.1175/1520-0469(1989)046<0163:TATERT>2.0.CO;2.
- Hendon, H. H., E. Lim, G. Wang, O. Alves, and D. Hudson (2009), Prospects for predicting two flavors of El Niño, *Geophys. Res. Lett.*, *36*(19), L19713, doi:10.1029/2009GL040100.
- Hlinka, J., D. Hartman, N. Jajcay, M. Vejmelka, R. Donner, N. Marwan, J. Kurths, and M. Paluš (2014), Regional and inter-regional effects in evolving climate networks, *Nonlin. Processes Geophys.*, *21*(2), 451–462, doi:10.5194/npg-21-451-2014.
- Hu, Z.-Z., A. Kumar, B. Jha, W. Wang, B. Huang, and B. Huang (2011), An analysis of warm pool and cold tongue El Niños: Air–sea coupling processes, global influences, and recent trends, *Clim. Dyn.*, *38*(9–10), 2017–2035, doi:10.1007/s00382-011-1224-9.
- Johnson, N. C. (2013), How many ENSO flavors can we distinguish?, *J. Clim.*, *26*(13), 4816–4827, doi:10.1175/JCLI-D-12-00649.1.
- Kao, H.-Y., and J.-Y. Yu (2009), Contrasting eastern-Pacific and central-Pacific types of ENSO, *J. Clim.*, *22*(3), 615–632, doi:10.1175/2008JCLI2309.1.
- Kim, H.-M., P. J. Webster, and J. A. Curry (2009), Impact of shifting patterns of Pacific Ocean warming on North Atlantic tropical cyclones, *Science*, *325*(5936), 77–80, doi:10.1126/science.1174062.
- Kim, W., S.-W. Yeh, J.-H. Kim, J.-S. Kug, and M. Kwon (2011), The unique 2009–2010 El Niño event: A fast phase transition of warm pool El Niño to La Niña, *Geophys. Res. Lett.*, *38*(15), L15809, doi:10.1029/2011GL048521.
- Kalnay, E., et al. (1996), The NCEP/NCAR 40-year reanalysis project, *Bull. Amer. Meteor. Soc.*, *77*(3), 437–471, doi:10.1175/1520-0477(1996)077<0437:TNYRP>2.0.CO;2.
- Kug, J.-S., and Y.-G. Ham (2011), Are there two types of La Niña?, *Geophys. Res. Lett.*, *38*(16), L16704, doi:10.1029/2011GL048237.
- Kug, J.-S., F.-F. Jin, and S.-I. An (2009), Two types of El Niño events: Cold tongue El Niño and warm pool El Niño, *J. Clim.*, *22*(6), 1499–1515, doi:10.1175/2008JCLI2624.1.
- Larkin, N. K., and D. E. Harrison (2005), Global seasonal temperature and precipitation anomalies during El Niño autumn and winter, *Geophys. Res. Lett.*, *32*(16), L16705, doi:10.1029/2005GL022860.
- Ludescher, J., A. Gozolchiani, M. I. Bogachev, A. Bunde, S. Havlin, and H. J. Schellnhuber (2013), Improved El Niño forecasting by cooperativity detection, *Proc. Natl. Acad. Sci. USA*, *110*(29), 11,742–11,745, doi:10.1073/pnas.1309353110.
- Ludescher, J., A. Gozolchiani, M. I. Bogachev, A. Bunde, S. Havlin, and H. J. Schellnhuber (2014), Very early warning of next El Niño, *Proc. Natl. Acad. Sci. USA*, *111*(6), 2064–2066, doi:10.1073/pnas.1323058111.
- McCormick, M. P., L. W. Thomason, and C. R. Trepte (1995), Atmospheric effects of the Mt. Pinatubo eruption, *Nature*, *373*(6513), 399–404, doi:10.1038/373399a0.
- Neelin, J. D. (2003), Tropical drought regions in global warming and El Niño teleconnections, *Geophys. Res. Lett.*, *30*(24), 2275, doi:10.1029/2003GL018625.
- Paluš, M., D. Hartman, J. Hlinka, and M. Vejmelka (2011), Discerning connectivity from dynamics in climate networks, *Nonlin. Processes Geophys.*, *18*(5), 751–763, doi:10.5194/npg-18-751-2011.
- Radebach, A., R. V. Donner, J. Runge, J. F. Donges, and J. Kurths (2013), Disentangling different types of El Niño episodes by evolving climate network analysis, *Phys. Rev. E*, *88*(5), 052807, doi:10.1103/PhysRevE.88.052807.
- Rasmusson, E. M., and T. H. Carpenter (1982), Variations in tropical sea surface temperature and surface wind fields associated with the Southern Oscillation/El Niño, *Mon. Wea. Rev.*, *110*(5), 354–384, doi:10.1175/1520-0493(1982)110<0354:VITSST>2.0.CO;2.
- Runge, J., V. Petoukhov, J. F. Donges, J. Hlinka, N. Jajcay, M. Vejmelka, D. Hartman, N. Marwan, M. Palu, and J. Kurths (2015), Identifying causal gateways and mediators in complex spatio-temporal systems, *Nat. Commun.*, *6*, 8502, doi:10.1038/ncomms9502.
- Saramäki, J., M. Kivelä, J.-P. Onnela, K. Kaski, and J. Kertész (2007), Generalizations of the clustering coefficient to weighted complex networks, *Phys. Rev. E*, *75*(2), 027105, doi:10.1103/PhysRevE.75.027105.
- Stolbova, V., P. Martin, B. Bookhagen, N. Marwan, and J. Kurths (2014), Topology and seasonal evolution of the network of extreme precipitation over the Indian subcontinent and Sri Lanka, *Nonlin. Processes Geophys.*, *21*(4), 901–917, doi:10.5194/npg-21-901-2014.
- Taschetto, A. S., and M. H. England (2009), El Niño Modoki impacts on Australian rainfall, *J. Clim.*, *22*(11), 3167–3174, doi:10.1175/2008JCLI2589.1.
- Tedeschi, R. G., I. F. A. Cavalcanti, and A. M. Grimm (2013), Influences of two types of ENSO on South American precipitation, *Int. J. Climatol.*, *33*(6), 1382–1400, doi:10.1002/joc.3519.
- Trenberth, K. E. (1997), The definition of El Niño, *Bull. Amer. Meteor. Soc.*, *78*(12), 2771–2777, doi:10.1175/1520-0477(1997)078<2771:TDOENO>2.0.CO;2.
- Tsonis, A. A., and K. L. Swanson (2008), Topology and predictability of El Niño and La Niña networks, *Phys. Rev. Lett.*, *100*(22), 228502, doi:10.1103/PhysRevLett.100.228502.
- Tsonis, A. A., K. L. Swanson, and P. J. Roebber (2006), What do networks have to do with climate?, *Bull. Amer. Meteor. Soc.*, *87*(5), 585–595, doi:10.1175/BAMS-87-5-585.
- Tsonis, A. A., K. L. Swanson, and G. Wang (2008), On the role of atmospheric teleconnections in climate, *J. Clim.*, *21*(12), 2990–3001, doi:10.1175/2007JCLI1907.1.
- Wang, Y., A. Gozolchiani, Y. Ashkenazy, and S. Havlin (2016), Oceanic El-Niño wave dynamics and climate networks, *New J. Phys.*, *18*(3), 033021, doi:10.1088/1367-2630/18/3/033021.
- Watts, D. J., and S. H. Strogatz (1998), Collective dynamics of small-world networks, *Nature*, *393*(6684), 440–442, doi:10.1038/30918.
- Wiedermann, M., J. F. Donges, J. Heitzig, and J. Kurths (2013), Node-weighted interacting network measures improve the representation of real-world complex systems, *Europhys. Lett.*, *102*(2), 28007.
- Wiedermann, M., J. F. Donges, D. Handorf, J. Kurths, and R. V. Donner (2015), Hierarchical structures in Northern Hemispheric extratropical winter ocean-atmosphere interactions, *arXiv:1506.06634 [physics]*, arXiv: 1506.06634.
- Yamasaki, K., A. Gozolchiani, and S. Havlin (2008), Climate networks around the globe are significantly affected by El Niño, *Phys. Rev. Lett.*, *100*, 228501, doi:10.1103/PhysRevLett.100.228501.

- Yeh, S.-W., J.-S. Kug, B. Dewitte, M.-H. Kwon, B. P. Kirtman, and F.-F. Jin (2009), El Niño in a changing climate, *Nature*, *461*(7263), 511–514, doi:10.1038/nature08316.
- Yuan, Y., and H. Yan (2012), Different types of La Niña events and different responses of the tropical atmosphere, *Chin. Sci. Bull.*, *58*(3), 406–415, doi:10.1007/s11434-012-5423-5.
- Zemp, D. C., M. Wiedermann, J. Kurths, A. Rammig, and J. F. Donges (2014), Node-weighted measures for complex networks with directed and weighted edges for studying continental moisture recycling, *Europhys. Lett.*, *107*(5), 58005, doi:10.1209/0295-5075/107/58005.